J. Fluid Mech. (1987), *vol.* 175, *pp.* 463–478
Printed in Great Britain

On the instability of sheared disturbances

By PETER H. HAYNES†
Joint Institute for the Study of the Atmosphere and the Ocean, University of Washington, Seattle, WA 98195, USA

(Received 23 July 1985 and in revised form 7 July 1986)

The equation for small-amplitude disturbances to an unbounded flow of constant shear on a beta-plane has well-known solutions of a particularly simple form. In physical terms such solutions represent a flow in which absolute-vorticity contours, initially taking a wavy configuration, are deformed by the basic-state shear. Here it is shown that, at least in cases where the initial disturbance has long wavelength, the vorticity distribution predicted by such solutions eventually becomes barotropically unstable, as the shearing over of material contours leads to local reversals in the cross-stream gradient of absolute vorticity.

1. Introduction

A multitude of authors working in a number of different areas of fluid dynamics, the first being Kelvin (Thomson 1887), have constructed what we shall refer to as sheared-disturbance solutions. These are time-dependent solutions of the equations for small-amplitude disturbances to a basic flow in which the shear is constant. The elemental forms of these solutions are single spatial Fourier modes in which the streamwise wavenumber remains constant and the cross-stream wavenumber changes at a constant rate. The effect of this change is that lines of constant phase are sheared over by the basic flow, almost as if they corresponded to contours of a passive tracer. (The correspondence is not always exact – see the remarks made in the next section.)

Here we shall be primarily concerned with sheared disturbances in a two-dimensional flow on a beta-plane, where there is a constant cross-stream gradient of planetary vorticity, as previously studied by Yamagata (1976), Boyd (1983) and Tung (1983). The new aspect of this work is that attention will be concentrated on the ultimate fate of the disturbances, particularly in the atmospherically relevant case when the viscosity is very small. A brief motivation for the study will be presented in the next section. The fluid-dynamical process exemplified by the sheared-disturbance solution is an ubiquitous one and it is therefore interesting that investigation of the flow represented by the solution raises the possibility that it may be unstable. Explicit confirmation of the instability is given by the results of a calculation described in §3 which derives growth rates and phase speeds for the unstable disturbances.

The way in which the instability arises is analogous to that found in other dynamical problems that have been studied very recently, the instability of a nonlinear Rossby-wave critical layer described by Killworth & McIntyre (1985) and Haynes (1985) being particularly closely related. Comparison with this problem

† Present address: Department of Applied Mathematics and Theoretical Physics, University of Cambridge, Silver Street, Cambridge, CB3 9EW, UK.

allows, amongst other things, an assessment of the extent to which the sheared disturbances are likely to be disrupted by the action of the instability. These qualitative considerations, and the results of the instability analysis itself, are confirmed by some simple numerical experiments described in §4.

2. The sheared-disturbance solution

The equation to be solved is that for unbounded two-dimensional incompressible flow on a beta-plane and is given by

$$\frac{\partial q}{\partial t}+J(\psi,q)=0, \tag{2.1}$$

where q is the absolute vorticity and ψ is a stream function. Cartesian coordinates x and y are used to describe spatial variation, and the velocity components in the x- and y-directions are given by $(\partial\psi/\partial x, -\partial\psi/\partial y)$. The absolute vorticity is defined by

$$q=\beta y+\frac{\partial v}{\partial x}-\frac{\partial u}{\partial y}=\beta y+\nabla^2\psi, \tag{2.2}$$

where β is the gradient of the background planetary vorticity, which is taken to be parallel to the y-axis. We consider a basic flow in the x-direction with constant shear Λ, which is here, without loss of generality, taken to be positive. This flow is weakly disturbed so that the total stream function may be written as

$$\psi=-\tfrac{1}{2}\Lambda y^2+\epsilon\phi(x,y,t). \tag{2.3}$$

The parameter ϵ is a dimensionless measure of the amplitude of the disturbance and is taken to be small. It is convenient from now on to work in terms of dimensionless variables defined using Λ/β as a lengthscale, Λ^{-1} as a timescale, Λ as a vorticity scale and Λ^3/β^2 as a scale for the stream function. Using (2.2) and (2.3) the dimensionless form of (2.1) may be written as

$$\left(\frac{\partial}{\partial t}+y\frac{\partial}{\partial x}\right)\nabla^2\phi+\frac{\partial\phi}{\partial x}=-\epsilon J(\nabla^2\phi,\phi), \tag{2.4}$$

which at leading order in ϵ is linear in ϕ. Let us consider the simplest possible case, in which the relative vorticity pattern at $t=0$ is given by

$$\zeta=\epsilon\nabla^2\phi=\epsilon\,\mathrm{Re}\{\exp(\mathrm{i}\kappa x+\mathrm{i}\lambda y)\}, \tag{2.5}$$

representing a single Fourier mode in x and y with dimensionless wavenumber (κ,λ), where κ is taken to be positive.

If ϵ is small enough it is plausible that the term on the right-hand side of (2.4) may be neglected. The resulting linear equation may be solved by a transformation to so-called sheared coordinates, a method first used by Phillips (1966) for the internal-gravity-wave problem and first applied to the Rossby-wave case by Yamagata (1976). However the transformation is not strictly necessary; we may simply seek a solution of the form

$$\phi=\phi^{(t)}(x,y,t)=\mathrm{Re}\{f(t)\exp(\mathrm{i}\kappa(x-yt)+\mathrm{i}\lambda y)\}, \tag{2.6a}$$

$$\zeta=\zeta^{(t)}(x,y,t)=\mathrm{Re}\{-[\kappa^2+(\kappa t-\lambda)^2]f(t)\exp(\mathrm{i}\kappa(x-yt)+\mathrm{i}\lambda y)\}, \tag{2.6b}$$

where the function $f(t)$ is to be determined. On substituting this expression into the equation we obtain an ordinary differential equation for $f(t)$ which, with the initial condition (2.5), may be solved and the answer substituted in (2.6a, b) to give

$$\phi^{(t)}(x,y,t) = \mathrm{Re}\left\{\frac{1}{\kappa^2+(\lambda-\kappa t)^2}\exp\left[\mathrm{i}\kappa(x-yt)+\mathrm{i}\lambda y+\frac{\mathrm{i}}{\kappa}\tan^{-1}\left(\frac{\kappa t-\lambda}{\kappa}\right)+\frac{\mathrm{i}}{\kappa}\tan^{-1}\left(\frac{\lambda}{\kappa}\right)\right]\right\}, \tag{2.7a}$$

$$\zeta^{(t)}(x,y,t) = \mathrm{Re}\left\{\exp\left[\mathrm{i}\kappa(x-yt)+\mathrm{i}\lambda y+\frac{\mathrm{i}}{\kappa}\tan^{-1}\left(\frac{\kappa t-\lambda}{\kappa}\right)+\frac{\mathrm{i}}{\kappa}\tan^{-1}\left(\frac{\lambda}{\kappa}\right)\right]\right\} \tag{2.7b}$$

(Yamagata 1976; Boyd 1983; Tung 1983). As first shown by Orr (1907) in the context of Couette flow (without the beta-effect), the modulus of the function f ultimately decreases but may initially increase if $\lambda < 0$. The possibility of temporary amplification, which is not affected by the inclusion of the beta-effect (Boyd 1983; Tung 1983), has been part of the reason for the recent interest in sheared disturbances in atmospheric flows (e.g. Farrell 1982). However, as Shepherd (1985) has pointed out, although the temporary amplification in one Fourier component may be considerable, when the initial disturbance is made up of a number of Fourier components the amplification of the disturbance as a whole is, more often than not, weak or non-existent.

One of the most revealing ways to present the solution is by displaying maps of absolute vorticity, which is conserved following material particles. Correct to $O(\epsilon^2)$, the absolute vorticity is given by

$$q = y+\epsilon\zeta^{(t)}(x,y,t). \tag{2.8}$$

Contours of q are shown in figure 1, for the case $\lambda = 0$, at times $t = 0$, 4 and 12, with the value of ϵ taken to be 0.25. Since ϵ has a finite value, there might seem to be a finite error involved in taking the solution of only the linear version of (2.4). However, as often turns out to be the case, the single plane wave is a finite-amplitude solution of the full nonlinear equation.

The progression seen from figure 1 (a–c) is mainly the result of the deformation of the material contours by the basic shear. This is not quite the whole explanation since the absolute vorticity is not a passive tracer and itself controls the flow field. However the effect of the induced circulations is merely to change the phase of the disturbance (Boyd 1983) through the Rossby-wave propagation mechanism. It is this which leads to the complex exponential factor in the expression for $f(t)$ included in the right-hand sides of (2.7a and b).

The maps of absolute vorticity make the mechanism behind the behaviour of sheared disturbances transparent. The amplitude of the vorticity perturbation (indicated by the meridional displacement of the contours) remains constant but, through the shearing action, the size of the spatial structure changes. In the case shown in figure 1 the scale shrinks, but in general there may be an initial period in which the scale grows, for example if the initial configuration of the contours were the mirror image of that in (c). The stream function is obtained by taking the inverse Laplacian of the vorticity field and so its amplitude decreases as the scale shrinks. At large times the absolute-vorticity field behaves more and more like a passive tracer since the induced circulations become weaker and weaker. One consequence of this is that the argument of the complex exponential factor in $f(t)$, which represents the phase change, approaches a constant value as t becomes large.

Of course, the absolute-vorticity field resulting from a *non*-plane wave initial

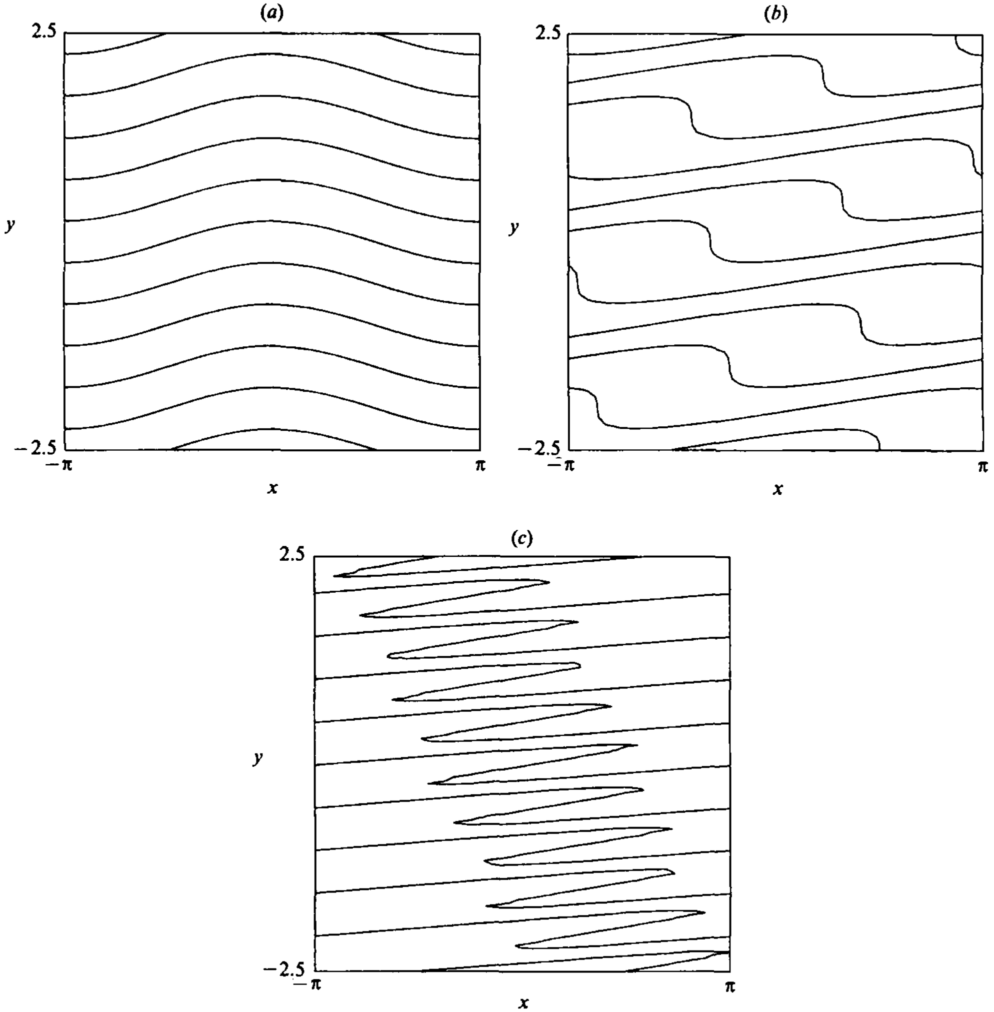

FIGURE 1. The absolute-vorticity distribution described by the sheared-disturbance solution with $\lambda = 0$ and $\epsilon = 0.25$ at (*a*) $t = 0$, (*b*) 4, (*c*) 12.

condition might look rather different to those shown in figures 1 (*a–c*), since it would comprise a superposition of solutions such as (2.7*b*). However, given the form such expressions take, it seems beyond question that the field would eventually be characterized by the local tilting of contours seen in figure 1 (*c*).

It is well known that sheared-disturbance solutions are closely related to the continuous part of the frequency spectrum of disturbances to shear flows (Orr 1907; Case 1960). Indeed solutions such as (2.7*a*, *b*) may be represented as a superposition of single-frequency modes, as one would expect if the spectrum was complete, but the representation is, not surprisingly, unwieldy. What is important, however, is that sheared disturbances form an essential part of the response of a shear flow to almost any forcing or disturbance (see Dickinson 1970 and Warn & Warn 1976 for one example). In the case of interest, two-dimensional flow on a beta-plane, where the essence of the dynamics is the advection of absolute vorticity, sheared disturbances result from any initial condition where absolute-vorticity contours do not lie along streamlines, as is the case in figure 1 (*a*). There is therefore good reason to believe that flow features similar to that represented by the sheared-disturbance solution are very common.

One of the striking features of the progression from figure 1 (*a–c*) is that the angle, measured in a clockwise direction, between portions of the absolute-vorticity contours and the x-axis increases so that, for example in figure 1 (*b*), certain tangents to the contours lie parallel to the y-axis. This is an indication that the local meridional vorticity gradients associated with the disturbance are as large as the basic-state absolute-vorticity gradient and might suggest, at first sight, that the term on the right-hand side of (2.4) can no longer be neglected. Of course in the single plane-wave case this term is identically zero. Furthermore, Tung (1983) was able to show that, under certain circumstances, even when the disturbances were not exactly plane waves the correction forced by the nonlinear term to the linear solution describing evolution from a bounded initial vorticity disturbance remained small, provided that it was small initially. The physical reason for this is that, for small-amplitude disturbances, by the time the meridional vorticity gradients have become as large as that in the basic state the meridional structure is very fine and the disturbances are, in effect, locally plane waves. Disturbance-vorticity contours and streamlines are then almost coincident (rather than being exactly coincident as they are in the exact plane-wave case). Tung (1983) deduced from his result that, if linear theory, i.e. ignoring the right-hand side of (2.4), was adequate to describe the initial evolution of the disturbance, then it would remain adequate for all time.

Now let us consider the absolute-vorticity gradient along a single meridional section, in figure 1 (*c*), for example. The fact that the absolute-vorticity contours have overturned indicates that the gradient is not one-signed. If the flow were unidirectional then Rayleigh's criterion for barotropic instability would be satisfied. Following Killworth & McIntyre (1985), who noted similar features in a nonlinear Rossby-wave critical layer, it is suggested that the sheared-disturbance flow is unstable.

3. The instability analysis

We now consider the evolution of small disturbances to the basic state comprising the uniform shear flow plus the sheared disturbance. We first take account of the fact that we are primarily interested in times when the meridional gradient of absolute vorticity is no longer one-signed. Differentiation of the expression for the vorticity field with respect to y shows that this is so only when $t = 0(\epsilon^{-1}\kappa^{-1})$. At such a time there is very fine structure (on a scale ϵ) in the sheared-disturbance vorticity field. Anticipating a multiple-scales approach to the problem, we define a slow timescale and a rapid spatial scale, described by the variables

$$\tau = \epsilon t, \quad Y = \epsilon^{-1} y. \tag{3.1}$$

For the time being we shall not introduce these new variables into the analysis explicitly.

Order-of-magnitude considerations suggest that the growth rate of the instability is likely to be roughly equal to the vorticity contrast $\epsilon\Lambda$ across the regions of positive and negative vorticity gradient so that the amplitude of the disturbance is likely to be a function of the slow time variable τ. However the disturbance may translate with some phase speed c_0, say, and any assumed functional form must allow this.

Therefore, imposing an extra disturbance on the flow which gives a contribution $\tilde{\epsilon}\tilde{\phi}$ to the stream function, the absolute vorticity may be written as

$$q = y + \epsilon\zeta^{(t)}(x, y, t) + \tilde{\epsilon}\nabla^2\tilde{\phi}(x - c_0 t, y, \epsilon^{-1} y, \epsilon t), \tag{3.2}$$

and the total stream function as

$$\psi - -\tfrac{1}{2}y^2 + \epsilon\phi^{(t)}(x, y, t) + \tilde{\epsilon}\tilde{\phi}(\kappa - c_0 t, y, \epsilon^{-1}y, \epsilon t). \tag{3.3}$$

The form of the new disturbance is restricted to varying on a lengthscale which is $O(1)$ in the x-direction. That this restriction allows the phenomena of interest to occur will become evident at the end of the calculation. The parameter $\tilde{\epsilon}$ is a measure of the amplitude of the vorticity perturbation associated with the extra disturbance. This would be as large as that associated with the sheared disturbance if $\tilde{\epsilon}$ were equal to ϵ. However, we shall take $\tilde{\epsilon} \ll \epsilon$, restricting the analysis to times when the new disturbance has not grown to sufficient amplitude to affect the sheared disturbance.

Substituting these expressions into the full equation (2.4), replacing ϵt, wherever it appears, by τ and using the fact that the sheared disturbance is itself a solution of the equation, we may obtain, at leading-order in ϵ, the equation for the new disturbance,

$$\left[\epsilon\frac{\partial}{\partial\tau} + (y - c_0)\frac{\partial}{\partial x}\right]\nabla^2\tilde{\phi} + \{1 + \tau\kappa\cos[\kappa(x - \epsilon^{-1}y\tau) + \lambda y]\}\frac{\partial\tilde{\phi}}{\partial x} = O(\epsilon^2). \tag{3.4}$$

The terms on the right-hand side of the equation turn out not to affect the leading-order solution and so at this stage will be set equal to zero. The basic-state absolute-vorticity gradient which appears as the coefficient of $\partial\tilde{\phi}/\partial x$ is a function of κx and $\kappa\tau$, and taking account of this variation turns out to be the main technical difficulty in solving the equation. However, when the non-dimensional zonal wave-number κ is such that $\kappa \ll 1$, this difficulty may be avoided. There is then a clear separation between the zonal lengthscales on which the sheared disturbance and the new disturbance vary, being in dimensional terms Λ/β and $\Lambda/\beta\kappa$ respectively. Furthermore there is a corresponding separation in the timescales, which are simply those for advection through the appropriate lengthscales.† This particular separation of scales is identical with that described in Killworth & McIntyre (1985) and may be exploited in the same manner. Thus in (3.4) the coefficient of $\partial\tilde{\phi}/\partial x$ may be regarded as being independent of x and τ; to reflect this we introduce the slow variables $\hat{\tau}$ and $\hat{x}$ defined by

$$\hat{\tau} = \kappa\tau, \quad \hat{x} = \kappa x, \tag{3.5}$$

which may be kept constant as x and τ vary by amounts of order unity.

We now seek normal-mode solutions of (3.4) taking the form

$$\tilde{\phi} = \mathrm{Re}\,[\hat{\phi}(y)\exp(\mathrm{i}\tilde{\kappa}(x - c_0 t - c\tau))], \tag{3.6}$$

where, without loss of generality, we may take $\tilde{\kappa} > 0$, and require that $\hat{\phi}$ be bounded as $|y| \to \infty$. The function $\hat{\phi}$ therefore satisfies the equation

$$(y - c_0 - \epsilon c)\left[\frac{\mathrm{d}^2\hat{\phi}}{\mathrm{d}y^2} - \tilde{\kappa}^2\hat{\phi}\right] + [1 + \hat{\tau}\cos(\hat{x} - y\hat{\tau}\,\epsilon^{-1} + \lambda y)]\,\hat{\phi} = 0. \tag{3.7}$$

We use a multiple-scales method to deal with the fine structure in the y-direction

† The relevant velocity scale is given by the shear Λ multiplied by a typical meridional particle displacement $\epsilon\Lambda/\beta$.

and so write y-derivatives as $\partial/\partial y = (\partial/\partial y)_Y + (1/\epsilon)(\partial/\partial Y)_y$, where Y is the variable defined in (3.1), and pose the expansions

$$\hat{\phi} = \hat{\phi}_0 + \epsilon \ln \epsilon \hat{\phi}_1 + \epsilon \hat{\phi}_2 + \epsilon^2 \ln \epsilon \hat{\phi}_3 + \epsilon^2 \hat{\phi}_4 + O(\epsilon^3 \ln \epsilon), \tag{3.8a}$$

$$\epsilon c = \epsilon c_2 + O(\epsilon^2), \tag{3.8b}$$

where each ϕ_n is a function of y and Y. The logarithmic terms are necessary because the leading-order approximation to (3.7) is singular when $y = c_0$.

These expansions may be substituted into (3.7) and the various powers of ϵ and $\ln \epsilon$ that appear may be isolated. The first four equations give that

$$\hat{\phi}_n = g_n(y), \quad n = 1,2,3,4, \tag{3.9}$$

where the functions g_n remain to be determined, but at $O(\epsilon^2)$ the equation

$$(y-c_0)\left[\frac{\mathrm{d}^2 g_0}{\mathrm{d}y^2} - \tilde{\kappa}^2 g_0\right] + [1 + \hat{r}\cos(\hat{x} - Y\hat{r} + \lambda y)]g_0 + (y-c_0)\frac{\partial^2 \hat{\phi}_4}{\partial Y^2} = 0 \tag{3.10}$$

is obtained. For there to be no terms growing like Y^2 the condition

$$(y-c_0)\left[\frac{\mathrm{d}^2 g_0}{\mathrm{d}y^2} - \tilde{\kappa}^2 g_0\right] + g_0 = 0 \tag{3.11}$$

must be satisfied, which gives an equation for g_0. This equation is simply that for a Rossby wave with phase speed c_0 on a flow with constant shear and in the presence of a *constant* gradient of absolute vorticity. What has emerged from the multiple-scales analysis is that, at least in the parts of the flow where the perturbation expansion (3.8*a*, *b*) is valid, the leading-order disturbance does not feel the rapid sinusoidal variations in the vorticity gradient.

Equation (3.11) has no solutions which are non-singular and satisfy the boundary conditions; however since c_0 is real it does have the singular solution

$$g_0 = A\mathrm{e}^{-\tilde{\kappa}(y-c_0)}\, U\left(-\frac{1}{2\tilde{\kappa}}, 0, \tilde{\kappa}(y-c_0)\right), \quad y > c_0 \tag{3.12a}$$

$$= B\mathrm{e}^{\tilde{\kappa}(y-c_0)}\, U\left(\frac{1}{2\tilde{\kappa}}, 0, -\tilde{\kappa}(y-c_0)\right), \quad y < c_0, \tag{3.12b}$$

where U is a confluent hypergeometric function as defined by Abramowitz & Stegun (1964). The singular behaviour of this solution near $y = c_0$ and the corresponding higher-order singularities in subsequent terms in the expansion (3.8*a*) lead to a breakdown of the assumed asymptotic form. It may be shown that the expansion is no longer valid when $y - c_0 = O(\epsilon)$, suggesting that this should be taken as an inner region and a new expansion for $\hat{\phi}$ posed. An inner coordinate $\tilde{Y} = (y-c_0)/\epsilon$ is therefore defined and the form of the new expansion valid in the inner region is taken to be

$$\hat{\phi} = \hat{\Phi}_0(\tilde{Y}) + \epsilon \ln \epsilon \hat{\Phi}_1(\tilde{Y}) + \epsilon \hat{\Phi}_2(\tilde{Y}) + O(\epsilon^2 \ln \epsilon). \tag{3.13}$$

From now on the analysis is very similar to that in the nonlinear critical layer problem analysed in Killworth & McIntyre (1985) (see especially their §3). Following the method of matched asymptotic expansions we shall require that the two expressions for $\hat{\phi}$, (3.8*a*) and (3.13), blend smoothly from one region to the other. To aid understanding of the physical nature of the problem which allows use of this mathematical formalism the different regions and scalings are shown in figure 2.

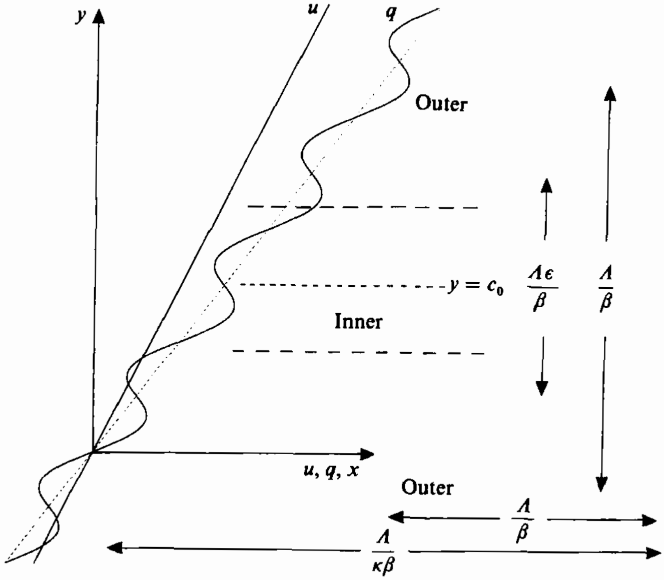

FIGURE 2. Regions for the matched-asymptotic analysis, together with the basic flow and basic-state absolute-vorticity profiles. The inner region is described by the coordinate Y and the outer region by the two coordinates y and $Y(=y/\epsilon)$. For the calculation presented in §3 the wavelength of the sheared disturbance $\Lambda/\beta\kappa$ is taken to be much larger than Λ/β.

Once again, this expansion (3.13) may be substituted into (3.7) and different orders of ϵ isolated. At $O(1)$ and $O(\epsilon \ln \epsilon)$ it is found that

$$\hat{\Phi}_0 = C_0, \quad \hat{\Phi}_1 = C_1, \tag{3.14}$$

where C_0 and C_1 are constants. Matching the first with the leading-order outer solution, using the power-series expansion of the function U given in Abramowitz & Stegun (1964), gives

$$C_0 = \frac{A}{\Gamma(-1/2\tilde{\kappa})} = \frac{B}{\Gamma(1/2\tilde{\kappa})}. \tag{3.15}$$

At next order the equation for $\hat{\Phi}_2$ is found to be

$$(\tilde{Y}-c_2)\frac{\partial^2\hat{\Phi}_2}{\partial \tilde{Y}^2}+[1+\hat{r}\cos(\hat{x}+\lambda c_0-\hat{r}\tilde{Y})]\,C_0 = 0. \tag{3.16}$$

The matching condition for the term proportional to $y-c_0$ in the expansion of the outer solution, which is valid as $(y-c_0)$ becomes small, may be written as

$$\left[\frac{\partial \hat{\Phi}_2}{\partial y}\right]_{y\to-\infty}^{y\to\infty} = -\pi C_0 \cot\frac{\pi}{2\tilde{\kappa}}. \tag{3.17}$$

This condition may be derived using the properties of the function U and a relation between digamma functions, all given in Abramowitz & Stegun (1964).

Evaluating the left-hand side of (3.17) using (3.16) the eigenvalue relation

$$\int_{-\infty}^{\infty} \frac{[1+\hat{r}\cos(\hat{x}+\lambda c_0-\hat{r}\tilde{Y})]}{\tilde{Y}-c_2}\,\mathrm{d}\tilde{Y} = \pi\cot\frac{\pi}{2\tilde{k}} \tag{3.18}$$

may be obtained (cf. (3.17) in Killworth & McIntyre 1985) where, since we are concerned with growing modes with $\mathrm{Im}(c_2) > 0$, the path of integration in the

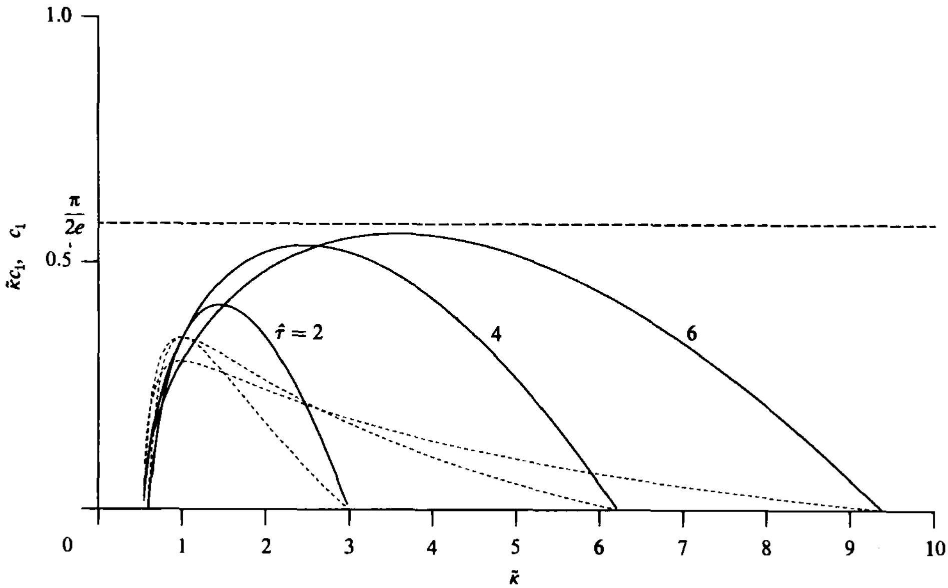

FIGURE 3. Sheared-disturbance stability problem: the imaginary part of the phase speed Im (c_2) (dotted line) and growth rate $\kappa\,\mathrm{Im}\,(c_2)$ (solid line), as predicted by (3.20), plotted against wavenumber κ. The cases $\hat{\tau} = 2, 4, 6$ are shown. The predicted large-τ value of Im (c_2), which is $\pi/2e$, is marked by a dashed line for comparison.

complex $\tilde{Y}$-plane is taken below the pole at $\tilde{Y} = c_2$. The value of the integral may be calculated using standard methods of contour integration and gives the real and imaginary parts of (3.18) to be

$$1+\hat{\tau}\exp\left(-\hat{\tau}\,\mathrm{Im}\,c_2\right)\cos\left(\lambda c_0-\hat{\tau}\,\mathrm{Re}\,c_2+\hat{x}\right) = 0, \tag{3.19a}$$

$$\hat{\tau}\exp\left(-\hat{\tau}\,\mathrm{Im}\,c_2\right)\sin\left(\lambda c_0-\hat{\tau}\,\mathrm{Re}\,c_2+\hat{x}\right) = 0. \tag{3.19b}$$

These equations may be solved to give

$$\mathrm{Im}\,c_2 = \frac{1}{\hat{\tau}}\ln\left[\hat{\tau}\sin\frac{\pi}{2\tilde{\kappa}}\right], \quad \mathrm{Re}\,c_2 = \frac{1}{\hat{\tau}}\left[c_0\lambda+\hat{x}-\tan^{-1}\left(\cot\frac{\pi}{2\tilde{\kappa}}\right)\right] \tag{3.20a, b}$$

Note that the quantities c_0 and $\mathrm{Re}\,(c_2)$ cannot be determined uniquely. The sheared-disturbance vorticity distribution is invariant under transformations $y = y+\Delta$, providing that $(\lambda-\hat{\tau}/\epsilon)\,\Delta = 2\pi N$, where N is an integer. This condition admits any Δ, at least to leading order in ϵ. The whole problem is then invariant under $y = y+\Delta$, $c = c+\Delta$, since the transformation in y may be accompanied by a Galilean transformation to take account of the shear flow. It is clear then that given one solution specified by the values of c_0 and c_2 there is an infinite family of solutions given by $c_0 = c_0+\Delta$, $c_2 = c_2+\lambda\Delta/\hat{\tau}$ where Δ is any real number.

The solution (3.20*a*) shows that growing normal-mode solutions exist if and only if $\hat{\tau} \geqslant 1$, which is just the condition for the absolute-vorticity gradient to change sign. In fact it is simple to prove a version of Rayleigh's theorem for this problem, in a manner analogous to that described in Haynes (1985).

The structure of $\mathrm{Im}\,(c_2)$ as a function of $\tilde{\kappa}$ is complicated near $\tilde{\kappa} = 0$ but the periodicity in $\tilde{\kappa}^{-1}$ means that the mode with the largest growth rate has $\tilde{\kappa} > \frac{1}{2}$. The quantities $\mathrm{Im}\,(c_2)$ and $\tilde{\kappa}\,\mathrm{Im}\,(c_2)$, the latter being the growth rate, are plotted against $\tilde{\kappa}$ for various values of $\hat{\tau}$ in figure 3.

When $\hat{\tau}$ is large it may be shown from (3.20*a*, *b*) that unstable modes exist for

$$\frac{1}{2}\left(1+\frac{1}{\pi\hat{\tau}}+O\left(\frac{1}{\hat{\tau}^3}\right)\right) < \tilde{\kappa} < \frac{\pi\hat{\tau}}{2}\left(1+O\left(\frac{1}{\hat{\tau}^2}\right)\right). \tag{3.21}$$

The fastest-growing wavenumber is then

$$\tilde{\kappa}_{\mathrm{m}} = \frac{\pi\hat{\tau}}{2e}\left(1+O\left(\frac{1}{\hat{\tau}^2}\right)\right), \tag{3.22}$$

for which the growth rate, $\kappa \operatorname{Im}(c_2)$, is given by

$$\tilde{\kappa}_{\mathrm{m}} \operatorname{Im}(c_2) = \frac{\pi}{2e}\left(1+O\left(\frac{1}{\hat{\tau}^2}\right)\right) \tag{3.23}$$

In dimensional terms the largest growth rate is of size $\epsilon\pi\Lambda/2e$ and the fastest-growing wavenumber is $\pi\hat{\tau}\beta/2e\Lambda$. Although the analysis up to this point has formally assumed that the dimensionless x-wavenumber of the sheared disturbance κ is small, the results might be expected to apply qualitatively if $\tilde{\kappa}_{\mathrm{m}} \operatorname{Im}(c_2)$ were larger than the rate of change of the sheared-disturbance solution, which is roughly given by τ^{-1}, and $\tilde{\kappa}_{\mathrm{m}}$ is larger than the wavenumber of the sheared-disturbance solution κ. These two conditions are always met for sufficiently large τ, suggesting that instability will eventually occur even when $\kappa \approx 1$. Of course, a more detailed analysis of the problem, including the x- and τ-variations in (3.4) could be performed, but, except for the numerical work discussed in the next section, lies outside the scope of this paper. The sheared disturbance has here been represented by the analytical solution (2.7*a*, *b*), this being the simplest possible case. However, the analysis may easily be extended to deal with sheared disturbances of a more general form, given by $\zeta^{(t)} = Z(x-yt, y, t)$, which in the long-time limit may be written as $\zeta^{(t)} = Z_0(x-Y\tau, y)$. It may be shown that unstable modes exist with their critical lines, $y = c_0$, in any region where $1+\tau(\partial Z_0/\partial x)(x-Y\tau, y)$ undergoes local reversals of sign. In particular this follows for those forms which have compact support and to which the analysis of Tung (1983) is applicable.

The linear instability analysis cannot, of course, predict the size to which unstable disturbances will ultimately grow. However, some insight into this question can be provided by results already obtained for the critical-layer instability mentioned earlier, which is believed to be very closely analogous. In both problems the disturbance is centred on a thin region in which there is a local reversal of the absolute-vorticity gradient and has an associated Rossby-wave structure (identical in each case) away from that region. The results presented for the critical-layer case by Haynes (1985) showed that the maximum displacement of fluid particles as the unstable disturbance grew was sufficient to rearrange drastically the local vorticity field, but tended to be limited to the lengthscale of the local reversals in absolute-vorticity gradient. It is plausible that the instability described in this paper evolves in a similar manner, so that only local (but nonetheless effective) rearrangement of the absolute vorticity takes place. The results of the numerical experiments to be described in the following section lend support to this hypothesis.

4. Simple numerical experiments

In order to provide an independent check on the predictions of the analysis in §3, it was decided to seek unstable behaviour in a numerical simulation. This also allowed the possibility of investigating flow configurations that do not satisfy the conditions under which the analysis of §3 is valid, namely $\kappa \ll 1$, $\tilde{\epsilon} \ll \epsilon \ll 1$, although it is emphasized that the purpose of this section is not to present an exhaustive study of the behaviour over wide ranges of the various flow parameters.

The numerical model is based on the barotropic vorticity equation (2.1), again in the dimensionless form (2.4) appropriate to disturbances to a shear flow, except that here ϵ is not required to be small. This equation is incremented in time using a semi-implicit method, the terms representing advection by the basic shear being approximated by the trapezoidal scheme and those representing advection by the disturbance by the Adams–Bashforth scheme.

In order to solve the Poisson equation for the stream function it was necessary to specify boundary conditions on ϕ at the edges of the domain. Clearly it is appropriate to choose the disturbance as being periodic in the x-direction. However the most appropriate choice of boundary conditions in the y-direction is less obvious. The sheared-disturbance solution is not periodic in the y-direction with any fixed period, L say. However we may impose that the *initial* perturbation to the shear flow (at $t = 0$) including both sheared disturbance and any extra disturbance is periodic, so

$$\phi(x, y, 0) = \phi(x, y+L, 0). \tag{4.1}$$

Then it may be shown that with such an initial condition solutions of (2.4) satisfy

$$\phi(x, y, t) = \phi(x+Lt, y+L, t). \tag{4.2}$$

This provides an adequate boundary condition for the Poisson equation, except for the zonal mean part, $\bar{\phi}(y, t)$ say. This may be determined by integrating the zonal momentum equation (obtained by taking the zonal mean of (2.4) and integrating with respect to y),

$$\frac{\partial}{\partial t}\left(\frac{\partial \bar{\phi}}{\partial y}\right) = \overline{\epsilon\phi\left(\frac{\partial^2 \phi}{\partial y^2} + \frac{\partial^2 \phi}{\partial x^2}\right)}, \tag{4.3}$$

where the overbar denotes the average over x, at a fixed value of y. Given the average of the vorticity over x, this determines $\bar{\phi}$ up to a constant, which is all that is required. The Poisson equation was solved using a Fourier transform method.

The model was tested in various ways. The treatment of the linear terms in (2.4) and the solution of the Poisson equation for the stream function were checked by successfully reproducing the sheared-disturbance solution, including the change of phase with time. The treatment of the nonlinear terms in (2.4) was checked by making the vorticity a passive tracer and comparing its advection by a fixed flow field with that predicted by an appropriate analytic solution. The resolution of the model and the size of the timesteps taken were chosen so that the differences between the numerical and analytic solutions represented, in each case, errors of less than 1 %.

Once the tests had given confidence that the program code contained no errors and that the numerical methods used were adequate, a number of numerical experiments were carried out. In each case (2.4) was solved with initial conditions of the form

$$\zeta = \nabla^2 \phi = a_0 \cos(\kappa_0 x + \lambda_0 y) + a_1 \cos(\kappa_1 x)\, \mathrm{e}^{-y^2}. \tag{4.4}$$

The first term in this expression was intended to represent the sheared disturbance, which was allowed to evolve in time and was not 'frozen'. The constant λ_0 was chosen to be negative, and large enough that the absolute-vorticity gradient in the y-direction, equal to $1 + \zeta_y$, would not be one-signed, since such cases were of primary interest, given the results obtained in §3. Choosing initial conditions such that the gradient was one-signed and then integrating in time for long enough that reversals appeared seemed an unnecessarily extravagant use of computing resources. For

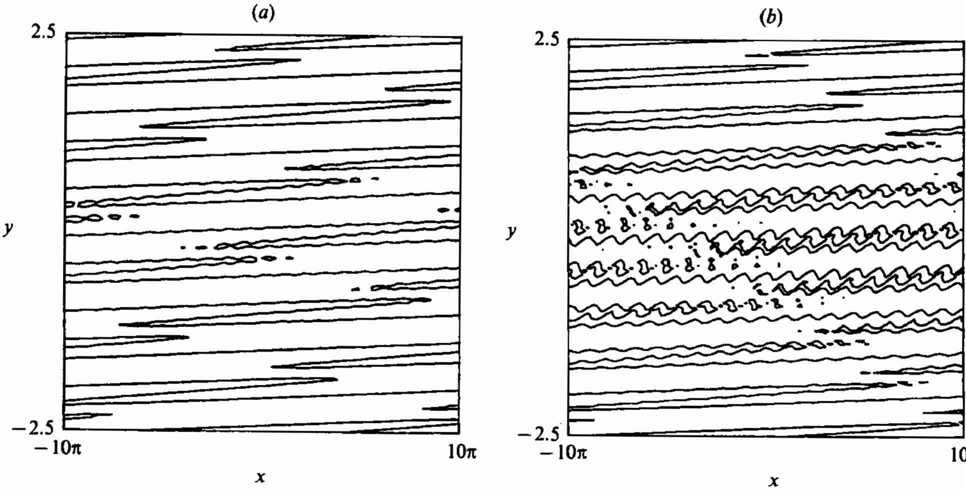

FIGURE 4. Contours of absolute vorticity in experiment (i) at (a) $t = 1$ and (b) 30. The contour interval is 0.5.

similar reasons, rather than waiting for the effects of the instability to appear through the growth of numerical noise arising from rounding error, an extra disturbance was added as the second term on the right-hand side of (4.4). The constant a_1 was chosen such that $|a_1| \ll |a_0|$, making this term initially small. The analysis of §3 suggests that under suitable conditions this extra disturbance grows in magnitude until it disrupts the sheared disturbance.

The computation was performed on a domain of width $2\pi/\kappa_0$ in the x-direction and L in the y-direction. The initial vorticity field was assumed to be periodic in the y-direction. The constant λ_0 was therefore chosen such that $\lambda_0 L$ was an integral multiple of 2π and L was chosen to be large enough that the second term appearing on the right-hand side of (4.4) was very small near the edge of the domain.

The results of three simulations are now described in detail.

(i) $$L = 5, \quad a_0 = 0.2, \quad \kappa_0 = 0.1, \quad L\lambda_0 = -32\pi, \quad a_1 = 0.02, \quad \kappa_1 = 2$$

The parameters here are chosen to be such that the asymptotic analysis of §3 should be valid, at least qualitatively. However, for this very reason, the requirements on the numerical resolution are very demanding since the y-scale of the sheared disturbances is very fine and the wavelength of disturbances that might be expected to grow is considerably smaller than the width of the computational domain. Figure 4 shows the absolute-vorticity fields at $t = 1$ and 30. Although the model resolution is very high, with 129 points across the domain in the y-direction and 64 waves (i.e. 127 degrees of freedom) used to represent the variation in the x-direction, some of the details of the vorticity field shown at $t = 30$ are clearly artificial. Nevertheless, from $t = 0$ to 30 there has clearly been considerable growth of disturbances with a wavelength about 16 or 17 times shorter than the original sheared disturbance. The reason that these new disturbances are confined to a central band of the computational domain is simply that the initial disturbance was so confined (recall (4.4)). Although it is difficult to make direct comparison between the instability theory of §3 and the results of the numerical simulation, the growth rates estimated from the latter are broadly consistent with those calculated. And, significantly, no such growth was seen when the equations were integrated over the same length of time, but from

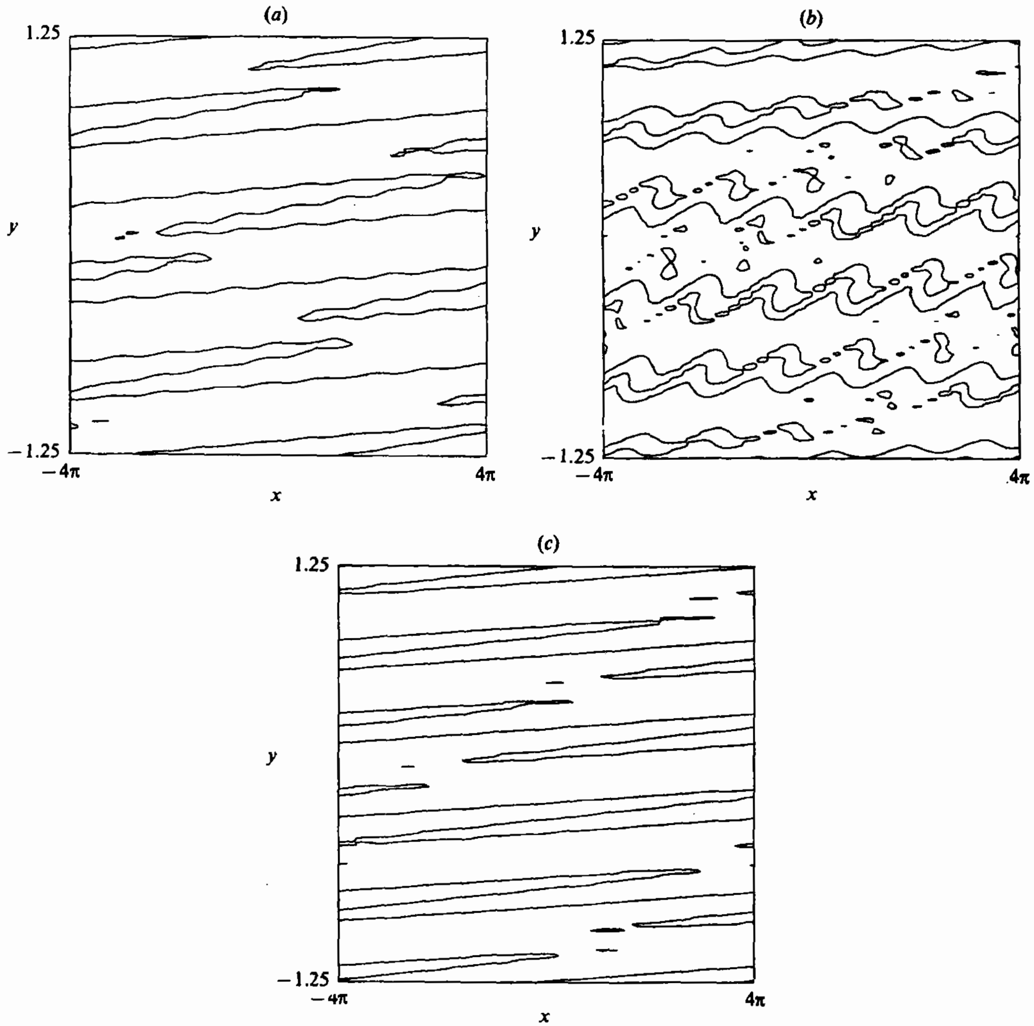

FIGURE 5. Contours of absolute vorticity in experiment (ii) at (*a*) $t = 0.4$ and (*b*) 36, and in the experiment repeated with nonlinear terms set to zero at (*c*) $t = 36$. The contour interval is 0.5.

an initial configuration in which $\lambda_0 = 0$, so the gradient of vorticity was everywhere one-signed. Therefore, taken together with arguments presented in §3 and the close similarity between aspects of figure 4(*b*) and equivalent pictures presented by Haynes (1985, figure 3) for the flow in a nonlinear Rossby-wave critical layer, the results of the numerical simulation provide very strong evidence for the local barotropic instability.

In addition, from the absolute-vorticity pattern shown in figure 4(*b*) we see that the particle displacement associated with the new disturbances has grown to a size comparable with the distance between the local reversals in the cross-stream vorticity gradient associated with the sheared disturbance. In the notation of the previous section the disturbance has grown to $O(\epsilon)$. The assumption of small amplitude which allowed the derivation of the linear disturbance equation (3.4) can no longer be valid and in this sense, at least, the disturbance has grown to finite amplitude. Whether the rearrangement of the vorticity across the width of the tongues can be judged to

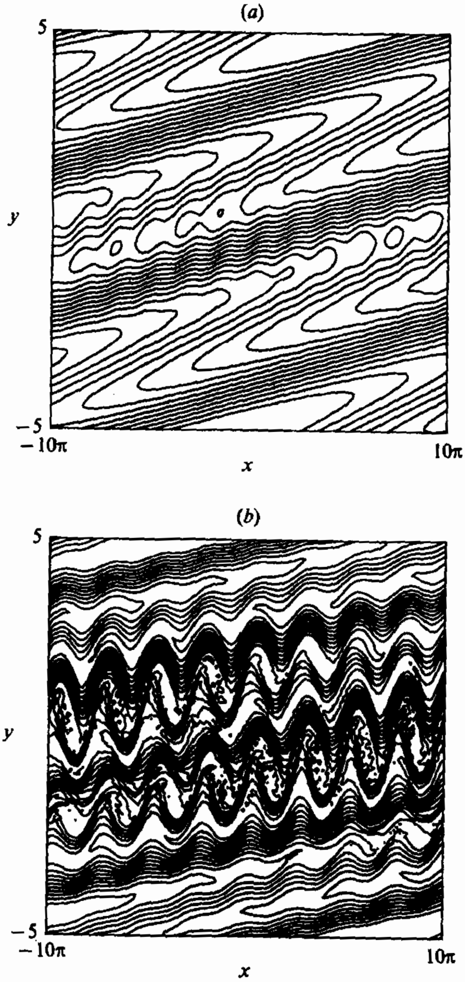

FIGURE 6. Contours of absolute vorticity in experiment (iii) at (a) $t = 11$ and (b) 19. The contour interval is 0.5.

be substantial and quasi-permanent is perhaps still open to question. It could, of course, be determined by running the model for a longer time, which would require even finer numerical resolution than was used in the case described here.

(ii) $L = 2.5, \quad a_0 = 0.2, \quad \kappa_0 = 0.25, \quad L\lambda_0 = -32\pi, \quad a_1 = 0.02, \quad \kappa_1 = 2$

In this case the zonal wavenumber of the sheared disturbance is not as small as in (i), so there is not such a clear division of scale between that and the disturbances which might grow through instability. Nevertheless from $t = 0.4$, shown in figure 5(a) to $t = 36$, in figure 5(b) there is again considerable growth in disturbances with a wavenumber of about 1.5. The growth rates in experiments (i) and (ii) are similar, as is to be expected from the analysis in §3, given than a_0 takes the same value in each case.

It is again emphasized that the fact that particle displacements associated with the disturbances are comparable with the distance between reversals in the vorticity gradient associated with the sheared disturbances suggests that the evolution is well past the regime in which the small-amplitude theory presented in §3 is valid.

For this case a 'linear' control experiment was performed with identical initial conditions but with terms appearing on the right-hand side of (2.4) set to zero. Figure 5(*c*) shows the vorticity distribution at $t = 36$. Comparison with figure 5(*b*) shows the striking qualitative difference in the evolution of the flow caused by the instability, and that this would be missed by a purely linear integration.

(iii) $L = 10, \quad a_0 = 2.0, \quad \kappa_0 = 0.1, \quad L\lambda_0 = 0, \quad a_1 = 0.2, \quad \kappa_1 = 2$

Here the sheared disturbance is of rather large amplitude so the small-ϵ assumption necessary for the calculation presented in §3 is not valid. However, as may be seen from figures 6(*a*) at $t = 11$, and 6(*b*) at $t = 19$, disturbances of similar character to those seen in (i) and (ii) grow to large enough amplitude to disrupt the vorticity field associated with the sheared disturbance completely.

5. Discussion

Using both analytical and numerical methods it has been shown that, when the parameter κ is small, sheared-disturbance solutions on a beta-plane represent flows which, for large enough times, are unstable to further disturbances. The instability is first possible after a time that is proportional to the reciprocal of the amplitude of the sheared disturbance. The result provides a mechanism by which the sheared disturbances might ultimately degrade that does not depend on any overtly dissipative process such as viscous diffusion. Furthermore, the instability is not allowed by a purely linear description, in which the right-hand side of the governing equation (2.4) is neglected. The assertion made by Tung (1983), that linear theory remains good if it is valid initially, must therefore be interpreted with caution, since the work presented here provides strong evidence that the linear 'sheared-disturbance' solutions are unstable. It appears that there is a tacit assumption in Tung's analysis which restricts the disturbances to having a cross-stream wavenumber in 'sheared coordinates' which is $O(1)$. The class of unstable disturbances identified in the last section tend to have a cross-stream wavenumber which is $O(1)$ in physical coordinates when t is $O(\epsilon^{-1})$ and therefore $O(\epsilon^{-1})$ in sheared coordinates. Furthermore, growing disturbances might well arise through random external forcing, which is outside the scope of Tung's analysis but is inevitably present in any flow, be it in the laboratory or in the atmosphere.

A problem that is closely related to that studied here is the classical one of two-dimensional Couette flow in the absence of a background planetary vorticity gradient, i.e. with $\beta = 0$. Clearly the non-dimensionalization used in §3 is not suitable for this problem, and the leading-order structure of the disturbances is different, especially in the outer region. Nevertheless, it turns out that the large-time discussion given in §3 is relevant even when $\beta = 0$. This may be confirmed by explicit calculation, but is made plausible by the fact that, even when $\beta \neq 0$, the variations in the vorticity gradient associated with the sheared disturbances become increasingly large compared to β as time increases.

So far we have been concerned with two-dimensional flow. However the results of the analysis in §3 might be applied directly to the mathematically identical problem of the evolution of disturbances to a flow with constant vertical shear, in the absence of horizontal boundaries, as described by the quasi-geostrophic equations. The regions where the potential-vorticity gradient would be alternately positive and negative would then form layers in the vertical and the resulting instability would be baroclinic rather than barotropic. Of course, a serious study of the baroclinic problem would have to address the effect of horizontal boundaries. Unfortunately there does not seem to be a simple analogue of the sheared-disturbance solution for a flow with rigid boundaries, except when $\beta = 0$, as considered by Farrell (1982) in the baroclinic case.

The instability studied here may be regarded as a very simple example of the class of what one might term 'tongue instabilities'. The common feature of the class is that the possibility of instability arises through the deformation of absolute-vorticity (or more generally potential-vorticity) contours in such a way that regions of opposing cross-stream gradient form on each side of an anomalously high- or low-vorticity tongue. Other very similar instabilities have recently come to light, the barotropic instability of a nonlinear Rossby-wave critical layer (Killworth & McIntyre 1985; Haynes 1985) being one example, and the baroclinic instability associated with tongues of high potential vorticity injected into the interior of an eddy-resolving ventilated ocean circulation model (Cox 1985) being another.

The analysis in §3 appeared in the author's Ph.D. thesis which was completed at the University of Cambridge. The numerical work and the preparation of the manuscript was supported by the Joint Institute for the Study of the Atmosphere and Ocean. The author is grateful to Drs W. Robinson and T. Shepherd and two anonymous referees for their valuable comments. This paper is JISAO contribution number 26.

REFERENCES

ABRAMOWITZ, M. & STEGUN, I. A. 1964 *Handbook of Mathematical Functions*. U.S. National Bureau of Standards.

BOYD, J. P. 1983 The continuous spectrum of linear Couette flow with the beta-effect. *J. Atmos. Sci.* **40**, 2304–2308.

CASE, K. M. 1960 Stability of inviscid plane Couette flow. *Phys. Fluids* **3**, 143–148.

COX, M. D. 1985 An eddy-resolving numerical model of the ventilated thermocline. *J. Phys. Oceanogr.* **15**, 1312–1324.

DICKINSON, R. E. 1970 Development of a Rossby wave critical level. *J. Atmos. Sci.* **27**, 627–633.

FARRELL, B. F. 1982 The initial growth of disturbances in a baroclinic flow. *J. Atmos. Sci.* **39**, 1663–1686.

HAYNES, P. H. 1985 Nonlinear instability of a Rossby-wave critical layer. *J. Fluid Mech.* **161**, 493–511.

KILLWORTH, P. D. & MCINTYRE, M. E. 1985 Do Rossby-wave critical layers absorb, reflect or over-reflect? *J. Fluid Mech.* **161**, 449–491.

ORR, W. M. F. 1907 The stability or instability of the steady motions of a perfect liquid and a viscous liquid: Parts I and II. *Proc. R. Irish Acad.* A**27**, 9–68; 69–138.

PHILLIPS, O. M. 1966 *Dynamics of the Upper Ocean*, 1st edn. Cambridge University Press.

SHEPHERD, T. G. 1985 On the time development of small disturbances to plane Couette flow. *J. Atmos. Sci.* **42**, 1868–1871.

THOMSON, W. 1887 Stability of fluid motion – rectilineal motion of viscous fluid between two parallel planes. *Phil. Mag.* **24**, 188–196.

TUNG, K. K. 1983 Initial-value problems for Rossby waves in a shear flow with critical level. *J. Fluid Mech.* **133**, 443–469.

WARN, T. & WARN, H. 1976 On the development of a Rossby wave critical level. *J. Atmos. Sci.* **33**, 2021–2024.

YAMAGATA, T. 1976 On trajectories of Rossby-wave packets released in a lateral shear flow. *J. Oceanogr. Soc. Japan* **32**, 162–168.